

Comparison of Direct and Flow Integration Based Charge Density Population Analyses

E. Francisco,* A. Martín Pendás, M. A. Blanco, and A. Costales

Departamento de Química Física y Analítica, Facultad de Química, Universidad de Oviedo, 33006-Oviedo, Spain

Received: July 24, 2007; In Final Form: September 13, 2007

Different exhaustive and fuzzy partitions of the molecular electron density (ρ) into atomic densities (ρ_A) are used to compute the atomic charges (Q_A) of a representative set of molecules. The Q_A 's derived from a direct integration of ρ_A are compared to those obtained from integrating the deformation density $\rho_{\text{def}} = \rho - \rho^0$ within each atomic domain. Our analysis shows that the latter methods tend to give Q_A 's similar to those of the (arbitrary) reference atomic densities ρ_A^0 used in the definition of the promolecular density, $\rho^0 = \sum_A \rho_A^0$. Moreover, we show that the basis set independence of these charges is a sign not of their intrinsic quality, as commonly stated, but of the practical insensitivity on the basis set of the atomic domains that are employed in this type of methods.

I. Introduction

Tens of methods have been proposed over the years to compute charges of atoms in molecules from first principles (see refs 1 and 2 and references therein). In most of these, charges are derived either from a partition of the orbital space^{3–8} or from a partition of the molecular electron density $\rho(\mathbf{r})$,^{9–12} although some of the methods that are commonly classified as belonging to the direct class may also be formulated within the second.¹³ Methods based on the partition of $\rho(\mathbf{r})$ may be further classified into exhaustive and nonexhaustive (fuzzy) depending on whether the real space is partitioned into exhaustive⁹ or overlapping¹⁰ atomic domains (Ω_A).

As known, the partition of space into atomic domains may be translated into the problem of choosing atomic weight functions $w_A(\mathbf{r})$ that provide a partition of the unity:¹²

$$\sum_A w_A(\mathbf{r}) = 1 \quad \forall \mathbf{r} \quad (1)$$

$w_A(\mathbf{r})$ is a stepwise function exactly 1 at any point \mathbf{r} within Ω_A and 0 elsewhere in exhaustive partitions, whereas it is a continuous function that usually takes a value very close to 1 near nucleus A and decays to 0 as we move away from it, in fuzzy partitions. The atomic density of atom A, $\rho_A(\mathbf{r})$, is defined in both cases as $\rho_A(\mathbf{r}) = w_A(\mathbf{r}) \rho(\mathbf{r})$. In direct integration methods (DIM), the electronic charge of atom A (N_A) is determined by integrating $\rho_A(\mathbf{r})$ within \mathbb{R}^3 .

Recently, a charge density analysis method called Voronoi deformation density (VDD)¹ has been proposed in which the atomic region of atom A is defined as the part of \mathbb{R}^3 closer to the nucleus of that atom than to any other nucleus (Voronoi cell). Moreover, N_A in the VDD method is obtained by computing the amount of charge that flows from/to a certain atomic region to/from other regions due to bond formation. This amounts to integrate the deformation density, defined as $\rho_{\text{def}}(\mathbf{r}) = \rho(\mathbf{r}) - \rho^0(\mathbf{r})$, where $\rho^0(\mathbf{r}) = \sum_A \rho_A^0(\mathbf{r})$ is the promolecular density and $\rho_A^0(\mathbf{r})$ is a reference atomic density for atom A, over the Voronoi cell of the atom. The VDD scheme is a particular case of a wider class of methods that we will call

flow integration methods (FIM) in which N_A is determined by integrating $w_A(\mathbf{r}) \rho_{\text{def}}(\mathbf{r})$ over \mathbb{R}^3 .

FIM methods have been praised in recent years for providing basis set independent, chemically meaningful atomic charges. Our aim in this paper is to critically ascertain the physical roots of such claims. On exploring integration methods against a redefinition of the $\rho_A^0(\mathbf{r})$'s, we will see that these charges are strongly dependent on the $\rho_A^0(\mathbf{r})$'s used to define the promolecular density, particularly in systems traditionally considered as highly ionic. The convergence properties of the atomic charges when the basis set is improved will also be investigated by taking the HCN molecule as a test example. Concerning this point, we claim that the almost basis set independent charges provided by some methods is due to the way in which these methods define the weights $w_A^0(\mathbf{r})$'s (nearly independent of the wave function quality), and not to their greater intrinsic quality.

We have organized the paper as follows. In section II we define different partitions of $\rho(\mathbf{r})$ into atomic densities and use them to derive expressions for the atomic charges within direct and flow integration methods. The computational details of the calculations that we have performed are given in section III. In section IV, we discuss the atomic charges obtained for a set of representative molecules according to the methods defined in section II. This discussion is preceded by an analysis of the basis set effects on the atomic charges of the HCN molecule. The main conclusions are summarized in section V.

II. Charge Density Partition and Atomic Charges: Direct and Flow Integration Methods

It is well-known that $\rho(\mathbf{r})$ always resembles the sum of isolated atomic densities. This fact has invited many to express $\rho(\mathbf{r})$ as a sum of atoms-in-the-molecule atomic densities, $\rho(\mathbf{r}) = \sum_A \rho_A(\mathbf{r})$, and to find the $\rho_A(\mathbf{r})$'s in several ways. The methods that we have actually used to perform this partition are described in subsection 2.1. They will be used in subsection 2.2 to determine the atomic charges using direct or flow integration methods.

A. Atoms-in-the-Molecule Existing Atomic Densities. It is possible to classify most of the $\rho_A(\mathbf{r})$'s roughly in four categories: topological densities, Hilbert-space partitioned

* Corresponding author. E-mail: evelio@carbono.quimica.uniovi.es.

densities, geometry-based densities, and densities that satisfy extremal conditions.

The best known and probably most realistic and physically meaningful topological space-partitioning method is that of Bader's theory of atoms in molecules (QTAIM).^{9,14} This provides an exhaustive partition of \mathbb{R}^3 in which the atomic regions are defined as the 3D attraction basins (Ω_A) of the gradient field of $\rho(\mathbf{r})$. Ω_A usually contains a single nucleus and is bounded by a zero local flux surface of $\nabla\rho$ ($\nabla\rho(\mathbf{r})\cdot\mathbf{n}(\mathbf{r}) = 0$ for $\mathbf{r} \in S(\Omega_A)$, where $\mathbf{n}(\mathbf{r})$ is a vector normal to the surface $S(\Omega_A)$). In terms of the $w_A(\mathbf{r})$'s the QTAIM partition may be recast as

$$w_A(\mathbf{r}) = \begin{cases} 1 & \text{if } \mathbf{r} \in \Omega_A \\ 0 & \text{elsewhere} \end{cases} \quad (2)$$

Concerning Hilbert-space partitioned densities, a recent partition of $\rho(\mathbf{r})$ into atomic components has been developed by Fernández Rico et al.^{7,8} In their approach, each $\rho_A(\mathbf{r})$ is determined by following a minimal deformation criterion (MinDef in what follows) of every two-center contribution to $\rho(\mathbf{r})$. Assuming that $\rho(\mathbf{r})$ is given in terms of primitive Gaussian functions $\phi_i(\mathbf{r})$ centered on the nuclei of the molecule

$$\rho(\mathbf{r}) = \sum_{ij} P_{ij} \phi_i(\mathbf{r}) \phi_j(\mathbf{r}) \quad (3)$$

(P_{ij} are the first-order density matrix coefficients) the final result is simple: every two-center (A and B) charge distribution is assigned to the nearest atom, except if it lies just in the middle of the A–B segment, which is half-and-half partitioned between both centers. Algebraically,

$$\rho_A(\mathbf{r}) = \sum_{ij} P_{ij}^A \phi_i(\mathbf{r}) \phi_j(\mathbf{r}) \quad (4)$$

$$P_{ij}^A = P_{ij} [m_A(i) \Theta(\zeta_{ij}) + m_A(j) \Theta(\zeta_{ji})] \quad (5)$$

where $m_A(i) = 1(0)$ if ϕ_i is (is not) A-centered, ζ_i is the ϕ_i exponent, $\zeta_{ij} = \zeta_i - \zeta_j$, and $\Theta(x)$ is the Heaviside step function ($\Theta(x>0) = 1$, $\Theta(x<0) = 0$, $\Theta(x=0) = 1/2$). It is easy to show that Mulliken's classical method can also be recast in the form as in eq 5 by choosing $P_{ij}^A = 0$, $P_{ij}/2$, P_{ij} depending if none, one (ϕ_i or ϕ_j), or both (ϕ_i and ϕ_j) basis functions are centered on A.

A geometric partition of $\rho(\mathbf{r})$ is the one inspired in Becke's partitioning of a general multicentered function $F(\mathbf{r})$ into atomic contributions,¹² defined by the following set of equations:

$$w_A(\mathbf{r}) = P_A(\mathbf{r}) \left| \sum_A P_A(\mathbf{r}) \right. \quad (6)$$

$$P_A(\mathbf{r}) = \prod_{B \neq A} \frac{1}{2} \left[1 - \frac{h[h[\dots h(v_{AB})]]}{k \text{ times}} \right] \quad (7)$$

$$h(v_{AB}) = (3v_{AB} - v_{AB}^3)/2 \quad (8)$$

$$v_{AB} = \mu_{AB} + a_{AB}(1 - \mu_{AB}^2) \quad (9)$$

$$\mu_{AB} = (r_A - r_B)/R_{AB} \quad (10)$$

$$a_{AB} = [(R_B/R_A) - (R_A/R_B)]/4 \quad (11)$$

where r_A (r_B) is the distance to atom A (B), R_{AB} denotes the internuclear distance between the nuclei of atoms A and B, and R_A and R_B are atomic size adjustable parameters. The $w_A(\mathbf{r})$ function defined by eq 6 is very close to 1 on nucleus A and

decays to zero on getting apart from this nucleus. This guarantees that $\rho_A(\mathbf{r})$ is associated to atom A. The stiffness of the cutoff between different atoms may be enhanced by increasing the parameter k that gives the number of times that the $h(v_{AB})$ polynomial is iterated to obtain $P_A(\mathbf{r})$ in eq 7. In the limit $k \rightarrow \infty$, the 3D space is exhaustively partitioned into disjoint atomic regions.

The last atomic density we will use is the classical stockholder or Hirshfeld partition,¹⁰ defined by

$$w_A(\mathbf{r}) = \rho_A^0(\mathbf{r})/\rho^0(\mathbf{r}) \quad (12)$$

where $\rho^0(\mathbf{r}) = \sum_A \rho_A^0(\mathbf{r})$ and $\rho_A^0(\mathbf{r})$ is a reference atomic density for the atom A. It can be shown^{15,16} that Hirshfeld's atoms minimize the Kullback–Leibler entropy deficiency functional,¹⁷

$$I = \sum_A \int \rho_A(\mathbf{r}) \ln \left(\frac{\rho_A(\mathbf{r})}{\rho_A^0(\mathbf{r})} \right) d\mathbf{r} \quad (13)$$

and are thus the ones best preserving the information contained in the ρ_A^0 's. If ρ_A^0 in eq 12 is chosen as the ground state spherically averaged density of neutral atoms A, $\rho^0(\mathbf{r})$ coincides with the promolecular density. Other possible choices of the reference densities will be explored in section IV.

B. Direct and Flow Integration Methods. A direct (DIM) or flow (FIM) integrated population analysis may be defined such that the total charge of atom A is obtained as

$$Q_A = Z_A - N_A = Z_A - \int_{\mathbb{R}^3} \rho_A(\mathbf{r}) d\mathbf{r} \quad (14)$$

(Z_A is the nuclear charge of atom A), and

$$Q_A = Q_A^0 - \int_{\mathbb{R}^3} w_A(\mathbf{r}) \rho_{\text{def}}(\mathbf{r}) d\mathbf{r} \quad (15)$$

respectively. In the last equation, ρ_{def} is the deformation density, defined as $\rho_{\text{def}} = \rho - \rho^0$, where $\rho^0 = \sum_A \rho_A^0$ and ρ_A^0 are (arbitrary) reference atomic densities. Equation 15 is a generalization of that used in the VDD method,¹

$$Q_A = - \int_{\text{Voronoi cell of A}} \rho_{\text{def}}(\mathbf{r}) d\mathbf{r} \quad (16)$$

which implicitly assumes that $\rho_A^0(\mathbf{r})$ corresponds to a neutral atom, i.e.

$$Q_A^0 = Z_A - N_A^0 = Z_A - \int_{\mathbb{R}^3} \rho_A^0(\mathbf{r}) d\mathbf{r} = 0 \quad (17)$$

and that $w_A(\mathbf{r})$ in eq 15 is chosen as 1 inside the Voronoi cell of atom A and 0 elsewhere. Notice that the DIM and FIM recipes provide two different sets of Q_A 's for a given density partition. It is worthwhile to remark that, whenever

$$\int_{\mathbb{R}^3} w_A(\mathbf{r}) \rho^0(\mathbf{r}) d\mathbf{r} = \int_{\mathbb{R}^3} \rho_A^0(\mathbf{r}) d\mathbf{r} = N_A^0 \quad (18)$$

Equation 15 becomes equal to eq 14 and there is no real difference between a FIM method and its DIM analogue. Hirshfeld's scheme (eq 12) clearly satisfies eq 18. Politzer's population analysis,¹⁸ where the $w_A(\mathbf{r})$'s are deliberately selected such that they define modified Voronoi polyhedra that partition the space into disjoint regions satisfying eq 18, provides another example in which this formal equivalence is valid whenever the reference atoms stay neutral ($N_A^0 = Z_A$).

TABLE 1: DIM and FIM Charge Density Analysis Methods Used in This Work for Several Weight Functions $w_A(\mathbf{r})$

$w_A(\mathbf{r})$	DIM	FIM
QTAIM	QTAIM	QTAIM-F
Becke ($R_A/R_B = 1, k = \infty$)		VDD
Becke ($R_A/R_B = 1, k = 3$)		fuzzy-VDD
Becke ($R_A/R_B = R_A^{\text{top}}/R_B^{\text{top}}, k = 3$)	Becke(T)	-
Fdez Rico et al.	MinDef	-
Hirshfeld	Hirshfeld	Hirshfeld

Many known charge density analysis methods may be obtained by combining a definition of the $w_A(\mathbf{r})$'s with eq 14 or eq 15. The methods actually used in this paper are defined in Table 1: The fuzzy-VDD method is a version of VDD in which the sharp Voronoi cell of atom A is smoothed by using $k = 3$ instead of $k = \infty$ in Becke's definition of $w_A(\mathbf{r})$. Becke-(T) is a direct integration method in which a Becke-like atomic partition defined in refs 13 and 19 is used. This definition is as follows: provided that a bond critical point exists between A and B, we will take R_A and R_B as R_A^{top} and R_B^{top} , the topological radii⁹ of atoms A and B, respectively; otherwise, R_A and R_B will be taken as the Bragg–Slater radii of atoms A and B taken from ref 20.

III. Computational Details

We have used the GAMESS code²¹ to obtain all the molecular wave functions in the ground electronic states and our PRO-MOLDEN code to determine the atomic charges. All numerical integrations were performed by using an angular Lebedev quadrature and a trapezoidal radial quadrature described in ref 22. To achieve an accuracy in the integrations of at least 1.0 me, β -spheres were required in the QTAIM atomic partition, with radii adjusted to 90% of the distance to the nearest interatomic surface intersection. The number of radial and angular points, both inside and outside the β -spheres, were varied until the required accuracy was obtained. The wave functions were obtained (except when it is explicitly indicated) from complete active space CAS[n,m] (n active electrons, m active orbitals) multiconfiguration calculations. The $\rho_A^0(\mathbf{r})$ were generated in the Hartree–Fock ground electronic states of the neutral or ionized atoms using the same basis as in the molecule, and spherically symmetrized before they were used in PRO-MOLDEN.

IV. Results and Discussion

In this section, we present and discuss the atomic charges obtained with the methods defined in section II. First, we analyze the basis set effects on the computed charges. For this purpose, we have taken the HCN molecule as a test example, although our results are general. Second, the results for the second-row AH_n saturated hydrides, the second-row diatomic molecules with 12, 14, and 20 electrons, several traditionally considered highly ionic molecules, the CH_3M ($M = \text{Li, Na, K}$) systems, and a set of representative charged molecules are discussed. These test examples cover a wide spectrum of charge transfers. Results from a wider set of molecules containing less polar bonds come to the same conclusions and will not be commented on here.

A. Basis Set Dependence on HCN. The restricted Hartree–Fock (RHF) charges for the carbon and nitrogen atoms of HCN using several basis sets are plotted in Figure 1. To avoid colateral effects on the results, the molecular geometry has been fixed to that obtained in a RHF/STO-3G minimization of the energy. First of all, the MinDef method, as Mulliken's classical

population analysis, shows the well-known basis set dependence. Aside from these Hilbert-space partitioned methods, we can see that, as soon as a d-type polarization function is added to the C and N atoms, the charges given by VDD, Hirshfeld, and QTAIM-F methods hardly change with the basis set. The effect of including a p-type function in the H basis or diffuse s,p-type functions is negligible in these three methods. The fuzzy-VDD results, not displayed in Figure 1, run parallel to those in its counterpart sharp version (VDD). It has been previously stated that the VDD and Hirshfeld methods yield very similar and almost neutral atoms.¹ This result is also reproduced here, where the C (N) atom charge is predicted marginally positive (negative) in both bases. QTAIM-F C and N charges ($\approx +0.20 e$ and $\approx -0.32 e$, respectively, when at least a d-type polarization function is included in the basis set) are slightly greater in absolute value than the VDD charges.

As we can see, QTAIM and Becke(T) charges appear very separated from the rest in Figure 1, being larger than in all the above methods. Before including a first d-type polarization function, the basis set dependence in these two methods is relatively pronounced. Nevertheless, contrarily to what is found when using MinDef charges, they converge to stable values when the basis set is improved. It is interesting, but not fortuitous, that Becke(T)'s charges almost run parallel to QTAIM's charges. The reason for this parallelism has to be searched in Becke(T)'s definition of atomic regions, crucially dependent on the atomic radii R_A used in their construction.¹⁹ For instance, a topological analysis of the electron density predicts an increase of R_N from 1.391 to 1.424 bohr and a decrease of R_C from 0.788 to 0.755 bohr in passing from the 6-311G(p) to the 6-311G(d) basis set. This produces an expansion of Becke(T)'s atomic region for N and, consequently, a gain of its electron population (that is, the N atom becomes more negative) in going from the 6-311G(p) to the 6-311G(d) basis set.

It is apparent from Figure 1 that the VDD and Hirshfeld methods, in which the atomic regions are determined by factors external to the wave function actually used in the calculation, give C and N charges nearly constant, even when a d-type function is included in the basis set. However, QTAIM, QTAIM-F, and Becke(T) charges only show a near basis set independence after using a d-type function in the calculation. In fact, the QTAIM atomic charges derived using as fixed atomic regions those determined from the topological analysis of the charge density corresponding to the RHF/6-31G calculation (QTAIM(*) in Figure 1) are less basis set dependent than the genuine QTAIM charges.

From these remarks we conclude that (1) the RHF charge density of HCN is practically converged by using a 6-311G(d) basis set, suffering a negligible change by further basis set improvements, and (2) the basis set independence of VDD and Hirshfeld charges¹ is not an intrinsic virtue of these two methods. Rather it arises as a consequence of (i) the fast convergence of the charge density as the wave function is improved and (ii) the wave function-free definition of the atomic regions in these two methods. This second conclusion is also supported by our results in other less polar molecules such as simple hydrocarbons or benzene. We believe that the goodness of a method should not be judged on the basis set independence of its results but on the convergence of these results to stable values when the accuracy of the wave function is increased. It is suspicious, for instance, that the Hirshfeld Q_A 's for large polarized basis sets are hardly distinguishable from those obtained from the unrealistic STO-3G density at a given geometry.

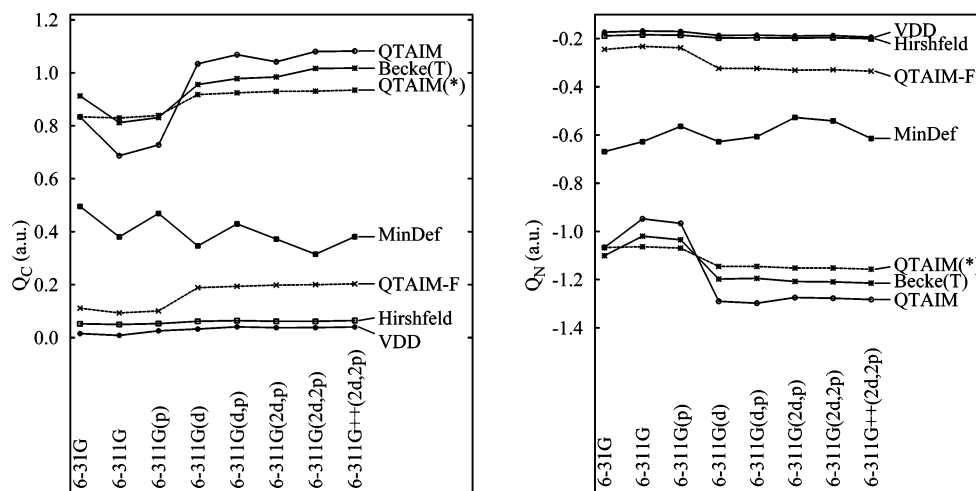


Figure 1. Basis set dependence of Q_C and Q_N (au) in HCN according to different methods defined in the text. The molecular geometry has been fixed to that obtained in a RHF/STO-3G energy minimization. QTAIM(*) atomic charges were obtained using the 6-31G interatomic surface with the rest of basis sets. The promolecular density, necessary in VDD, QTAIM-F, and Hirshfeld methods, is formed with the spherically averaged atomic densities of the neutral atoms.

TABLE 2: CASSCF//6-311G(d,p) Atomic Charges for the Second Row Hydrides

method	LiH (Q_{Li})	BeH ₂ (Q_{Be})	BH ₃ (Q_B)	CH ₄ (Q_C)	NH ₃ (Q_N)	H ₂ O (Q_O)	HF (Q_F)
MinDef	0.609	0.547	0.895	-0.247	-0.251	-0.381	-0.367
QTAIM	0.902	1.672	1.929	0.014	-0.983	-1.087	-0.717
Becke(T)	0.718	1.304	1.841	0.063	-0.719	-0.638	-0.414
Hirshfeld	0.388	0.353	0.191	-0.101	-0.270	-0.308	-0.226
VDD	0.446	0.392	0.232	-0.039	-0.221	-0.301	-0.238
fuzzy-VDD	0.418	0.337	0.196	-0.061	-0.228	-0.298	-0.233
QTAIM-F	0.265	0.115	0.175	-0.030	-0.266	-0.281	-0.179

B. Atomic Charges in Representative Molecules. We have performed CASSCF//6-311G(d,p) calculations on the second-row AH_n saturated hydrides including all the electrons in the active space and m active orbitals ($m = 6$ for LiH, $m = 7$ for BeH₂, $m = 8$ for BH₃, and $m = 9$ for CH₄, NH₃, H₂O, and HF). The results are collected in Table 2. As expected, the atomic charge of the second row atom decreases from LiH to HF in all the methods, being clearly positive for Li, Be, and B and negative for N, O, and F. The C atom is always the nearest to neutral in the sequence. For the QTAIM and Becke(T) partitions, Q_C is positive and small, though it is slightly negative in the other. Differences between the VDD and fuzzy-VDD schemes are rather small, and the fuzzy-VDD method, which requires less integration points than the VDD method to achieve a comparable accuracy, may be considered as an accurate alternative for the latter.

The similarity between the QTAIM and Becke(T) methods is of a different type. Provided that atoms A and B are bonded, the weight functions $w_A(\mathbf{r})$ and $w_B(\mathbf{r})$ in Becke(T)'s partition are close to 0.5 (exactly 0.5 for a diatomic molecule) at the point along the internuclear axis where $r_A/r_B = R_A^{\text{top}}/R_B^{\text{top}}$. As a result, the cutoff of the Becke ($k \rightarrow \infty$) region almost coincides with the bond critical point. Out but not very far from the A–B axis the points $w_A(\mathbf{r}) = 0.5$ will also be relatively close to the QTAIM interatomic surface,²³ so the similarities between both methods found in Table 2 stem from the deliberate choice of the atomic radii in Becke's method as equal to the topological ones.

From Table 2, it is clear that the QTAIM partition gives higher atomic charges than the Hirshfeld, VDD, fuzzy-VDD, and QTAIM-F methods. It has sometimes been suggested that this is a sign of the exaggerated ionicity predicted by the QTAIM method,¹ and that, due to this, and also to its alleged basis set dependence, a flow integration method, such as VDD, which

provides more “reasonable” charges and is less basis set dependent, would be preferable. Concerning the basis set dependence, we have already commented in subsection IV.A how the QTAIM charges converge to final stable values upon increasing the quality of the basis set, and also how the near basis set independence of VDD and Hirshfeld charges emerges, not from their intrinsic quality, but from the complete independence of the atomic weight functions $w_A(\mathbf{r})$ on the molecular wave function. Regarding the more “reasonable” charges provided by the VDD method, we want to stress a point that we believe is a serious disadvantage of this and other FIM schemes: its dependence on an arbitrary reference, resulting in different atomic charges with the same wave function when one changes the promolecular density $\rho^0(\mathbf{r})$. We analyze below this issue in more detail.

C. Relevance of the Reference Densities. We have collected in Table 3 the atomic charges for the second row diatomic molecules with 12, 14, and 20 electrons. The results corresponding to the VDD, fuzzy-VDD, and QTAIM-F methods were obtained by computing $\rho^0(\mathbf{r})$ either from the ρ_A^0 's of the neutral atoms or from the ρ_A^0 's of the monpositive (Na⁺, Li⁺, Mg⁺, Be⁺, Al⁺, B⁺, C⁺, Si⁺) and mononegative (F⁻, O⁻, N⁻, and C⁻) ions. These ionic references are standard in the thermochemistry of ionic systems, because multiply charged anions are usually not stable. Several revealing facts emerge from our results: (i) the atomic charges in the Hirshfeld, VDD, fuzzy-VDD, and QTAIM-F methods are quite dependent on the promolecular density used in the calculation; (ii) In LiF, BeO, NaF, MgO, and AlN, the charges of the metal when ρ^0 is built from the ρ_A^0 's of the neutral atoms are very small; (iii) The atomic charges in the above systems increase notably when the ρ_A^0 's of the ions are used. In LiF, BeO, NaF, and MgO, the Hirshfeld, VDD, fuzzy-VDD, and QTAIM-F charges are in fact

TABLE 3: Atomic Charges for the Second Row Diatomic Molecules^a

method	LiF (Li)	BeO (Be)	BN (B)	BF (B)	CO (C)	NaF (Na)	MgO (Mg)	AlN (Al)	SiC (Si)
MinDef	0.892	0.746	0.271	0.233	0.106	0.982	0.977	0.584	0.354
QTAIM	0.929	1.631	1.200	0.897	1.152	0.932	1.084	0.935	0.974
Becke(T)	0.829	1.238	1.078	0.879	1.130	0.865	0.929	0.915	1.044
Hirshfeld	0.589	0.541	0.170	0.069	0.059	0.657	0.478	0.236	0.144
	0.983	1.091	0.681	0.489	0.562	0.986	0.899	0.687	0.619
VDD	0.495	0.517	0.135	0.049	0.055	0.641	0.528	0.251	0.186
	0.929	0.977	0.595	0.455	0.515	0.966	0.898	0.662	0.605
fuzzy-VDD	0.530	0.496	0.130	0.023	0.038	0.599	0.488	0.222	0.154
	0.928	0.988	0.621	0.463	0.529	0.960	0.894	0.668	0.606
QTAIM-F	0.191	0.502	0.198	-0.056	0.040	0.535	0.504	0.267	0.207
	0.982	1.179	0.709	0.383	0.538	0.982	0.916	0.680	0.636

^a Calculations are CASSCF[8,8]/TZV(d) and CASSCF[10,10]/TZV(d) for the (12,20) and 14 isoelectronic series, respectively. The first (second) entry in Hirshfeld, VDD, fuzzy-VDD, and QTAIM-F methods uses as $\rho_A^0(\mathbf{r})$ to construct the promolecular density, $\rho^0(\mathbf{r})$, the corresponding to the neutral atoms (monopositive and mononegative ions).

TABLE 4: Atomic Charges for Several Molecules Widely Recognized as Highly Ionic^a

molecule/atom	QTAIM	Hirshfeld	VDD	QTAIM-F
LiH/Li	0.911	0.413	0.474	0.259
		0.991	0.972	1.000
NaH/Na	0.810	0.413	0.509	0.452
		0.977	0.950	0.957
NaCl/Na	0.918	0.626	0.622	0.498
		0.982	0.931	0.977
BeF ₂ /Be	1.807	0.638	0.524	0.090
		1.950	1.712	1.931

^a First (second) entry numbers have been obtained using the Li⁰H⁰, Na⁰H⁰, Na⁰Cl⁰, and Be⁰F⁰ (Li⁺H⁻, Na⁺H⁻, Na⁺Cl⁻, and Be²⁺F⁻) ρ_A^0 's.

fairly close to the QTAIM values. It seems that for these molecules all the methods offer results more consistent with each other when the ρ_A^0 's of the ions are used. Our results also support the following conclusion: atomic charges derived from flow integration methods are not necessarily small. Rather, they have a tendency to give values very similar to those of their reference counterparts.

We can clearly appreciate this in Table 4, where we have collected the RHF atomic charges for the positive atoms of some molecules, widely accepted as largely ionic. In all of the cases, the Hirshfeld, VDD, and QTAIM-F charges are very low when the ρ_A^0 's of the neutral atoms are used. However, all of them increase noticeably, becoming very similar to the QTAIM values, when the ρ_A^0 's of the monopositive and mononegative ions are employed. The case of BeF₂ is particularly striking. In this molecule, the Be atomic charge passes from about 0.09–0.64 *e* to 1.71–1.95 *e* in going from the Be⁰F⁰ to the Be²⁺F⁻ ρ_A^0 's.

The tendency of flow integration methods to predict atomic charges resembling those of their parent ρ_A^0 's is not exclusive of molecules formed by two very different electronegative atoms. In Table 5 we present a summary of the results obtained for the CH₃M (M = Li, Na, K) molecules when ρ^0 is computed either from the ρ_A^0 of the neutral atoms or from the ρ_A^0 of the monopositive (M⁺) and mononegative (C⁻) ions (and neutral H atoms). We observe again the non-uniqueness of Hirshfeld, VDD, and QTAIM-F charges. These three methods give metallic charges fairly close to the QTAIM values when ionic ρ_A^0 's are used to construct ρ^0 and much smaller when ρ^0 is obtained from the ρ_A^0 's of the neutral atoms. It is also interesting to remark that the C charges in this case are very similar in the three hydrides and, within a given hydride, in the three flow integration methods.

TABLE 5: RHF/TZV++(d,p) Atomic Charges for C and M Atoms in the CH₃M (M = Li, Na, K) Molecules^a

	CH ₃ Li		CH ₃ Na		CH ₃ K	
	C	Li	C	Na	C	K
QTAIM	-0.572	0.912	-0.466	0.803	-0.454	0.852
Becke(T)	-0.315	0.753	-0.216	0.675	-0.230	0.790
Hirshfeld	-0.416	0.511	-0.388	0.503	-0.440	0.609
	-1.118	0.968	-1.074	0.924	-1.024	0.895
VDD	-0.220	0.388	-0.216	0.435	-0.281	0.547
	-1.139	0.802	-1.110	0.790	-1.118	0.870
QTAIM-F	-0.144	0.252	-0.294	0.432	-0.352	0.520
	-1.216	0.962	-1.121	0.873	-1.077	0.892

^a ρ^0 in the first (second) entry is built from the ρ_A^0 's of the neutral atoms (neutral H atom, and C⁻ and M⁺ ions).

TABLE 6: Atomic Charges for the OH⁻, H₃O⁺, NO₃⁻, NH₄⁺, and CN⁻ Molecules at Their RHF Equilibrium Geometries^a

molecule	ρ^0	atom	QTAIM	Hirshfeld	VDD	QTAIM-F
OH ⁻	O ⁰ H ⁰	O	-1.434	-0.940	-0.898	-1.051
OH ⁻	O ⁻ H ⁰	O		-1.105	-1.160	-1.120
OH ⁻	O ⁰ H ⁻	O		-0.499	-0.568	-0.376
H ₃ O ⁺	O ⁰ H ⁰	O	-1.275	0.087	-0.019	0.389
H ₃ O ⁺	O ⁻ H ⁰	O		-0.134	-0.656	0.281
NO ₃ ⁻	O ⁰ N ⁰	O	-0.677	-0.424	-0.467	-0.463
NO ₃ ⁻	O ⁻ N ⁰	O		-0.570	-0.601	-0.578
NO ₃ ⁻	O ⁰ N ⁻	O		-0.229	-0.269	-0.250
NH ₄ ⁺	N ⁰ H ⁰	N	-1.124	0.091	-0.004	0.231
NH ₄ ⁺	N ⁻ H ⁰	N		-0.191	-0.811	-0.047
CN ⁻	C ⁰ N ⁰	C	0.763	-0.480	-0.448	-0.303
CN ⁻	C ⁻ N ⁰	C		-0.770	-0.746	-0.727
CN ⁻	C ⁰ N ⁻	C		-0.188	-0.225	-0.184

^a The basis set is 6-311G++(d,p) except in OH⁻ which is TZV++(2d,p).

As final test examples, we have determined the atomic charges for several charged molecules (OH⁻, H₃O⁺, NO₃⁻, NH₄⁺, and CN⁻) using the QTAIM method and three flow integration schemes (Hirshfeld, VDD, QTAIM-F) with different choices of ρ^0 . Our results are gathered in Table 6. Several interesting facts stand out. The QTAIM O atomic charge in OH⁻, H₃O⁺, and NO₃⁻ is more negative than in the three flow integration methods. Moreover, the O atomic charge in the latter schemes changes considerably with the promolecular density. The O atomic charge in OH⁻, H₃O⁺, and NO₃⁻ molecules becomes more negative in passing from a O⁰ ρ_A^0 to a O⁻ ρ_A^0 . This also occurs with the N atomic charge in NH₄⁺ and the C atomic charge in CN⁻. These numbers show again the tendency of flow integration methods to give charges as close as possible to those of their atomic references. Another deficiency of these schemes is that, even using the same ρ_A^0 for a given atom, its

atomic charge in the molecule depends on the ρ_A^0 's employed for the rest of the atoms. This may be clearly seen in Table 6 by comparing (i) the O charge in OH⁻ using O⁰H⁰ and O⁰H⁻ ρ_A^0 's, (ii) the O charge in NO₃⁻ using O⁰N⁰ and O⁰N⁻ ρ_A^0 's, and (iii) the C charge in CN⁻ using C⁰N⁰ and C⁰N⁻ ρ_A^0 's. In all of the cases, the charge is less negative (significantly so in CN⁻) when using a negative counteratom ρ_A^0 .

Upon this scenario we clearly disapprove the use of flow integration methods to derive atomic charges. If selected, however, we may wonder which are the best ρ_A^0 's to be used. We believe that an unambiguous criterion may be constructing the promolecular density using the ρ_A^0 's that provide a minimum loss of information (in the sense of a minimum value of the Kullback–Leibler entropy deficiency I , eq 13) upon molecule formation. Preliminary results in largely ionic molecules have shown that I is much smaller when ions instead of neutral atoms are used to construct the ρ_A^0 's. As we have seen in LiF, BeO, NaF, and MgO, FIM charges derived in that case are relatively close to the QTAIM values.

V. Conclusions

In this work, we have compared the performance of population analyses corresponding to several partitions of the molecular electron density, $\rho(\mathbf{r})$, into atomic densities, $\rho_A(\mathbf{r})$, with the help of the atomic weight functions $w_A(\mathbf{r})$. These functions may be either discontinuous or continuous, providing an exhaustive or a fuzzy partition of the physical space, respectively. Two different types of methods (direct integration methods and flow integration methods) have been established, and a closed unified expression for the atomic charges in both of them has been given in terms of the $w_A(\mathbf{r})$'s.

These two types of schemes have been compared to each other by computing the atomic charges of the second-row AH_{*n*} hydrides, second-row diatomic molecules with 12, 14, and 20 electrons, some small highly ionic molecules, the CH₃M (M = Li, Na, K) systems, and five simple molecular ions. Our analysis shows that flow integration methods suffer from a very undesirable property. They provide atomic charges that are similar to those of the reference atomic densities employed in the definition of their promolecular density. This means that they are not univocally determined from the molecular wave function, and the same wave function will yield different atomic charges with different promolecule definitions. It is our opinion that a well-defined molecular wave function should always provide a unique set of atomic charges. We thus believe that the non-uniqueness of the atomic charges for a fixed molecular wave function is a very critical disadvantage of flow integration methods. Consequently, we do not recommend using these population analyses.

On the other hand, the purportedly poor quality of QTAIM charges claimed in ref 1, due to their basis set dependence and the “too ionic” molecules they provide, is a flawed conclusion. QTAIM charges do obviously depend on the quality of the basis set (just in the same way as it happens with quantum-mechanical observables as the total energy) but reach final stable values in the infinite basis set limit. Moreover, contrary to atomic charges derived from flow integration methods, QTAIM atomic charges are univocally defined. The goodness of a charge density population analysis lies on the physical principles it is based on, and also on its internal consistency. In this sense, the outstanding physical principles on which the QTAIM is based make us advocate the use of the atomic charges derived from this theory.

Acknowledgment. Financial support from the Spanish MEC, Project No. CTQ2006-02976, and the ERDF of the European Union, is acknowledged.

References and Notes

- (1) Fonseca-Guerra, C.; Handgraaf, J. W.; Baerends, E. J.; Bickelhaupt, F. M. *J. Comput. Chem.* **2003**, *25*, 189.
- (2) Bader, R. F. W.; Matta, C. F. *J. Phys. Chem.* **2004**, *108*, 8385.
- (3) Mulliken, R. S. *J. Chem. Phys.* **1955**, *23*, 1833.
- (4) Mulliken, R. S. *J. Chem. Phys.* **1955**, *23*, 1841.
- (5) Mulliken, R. S. *J. Chem. Phys.* **1955**, *23*, 2338.
- (6) Mulliken, R. S. *J. Chem. Phys.* **1955**, *23*, 2343.
- (7) Fernández-Rico, J.; López, R.; Ramírez, G. *J. Chem. Phys.* **1999**, *110*, 4213.
- (8) Fernández-Rico, J.; López, R.; Ema, I.; Ramírez, G. *J. Chem. Phys.* **2002**, *117*, 533.
- (9) Bader, R. F. W. *Atoms in Molecules*; Oxford University Press: Oxford, U.K., 1990.
- (10) Hirshfeld, F. L. *Theor. Chim. Acta* **1977**, *44*, 129.
- (11) Li, L.; Parr, R. G. *J. Chem. Phys.* **1986**, *84*, 1704.
- (12) Becke, A. D. *J. Chem. Phys.* **1988**, *88*, 2547.
- (13) Martín Pendás, A.; Blanco, M. A.; Francisco, E. *J. Comput. Chem.* **2007**, *28*, 161.
- (14) Bader, R. F. W.; Beddall, P. M. *J. Chem. Phys.* **1972**, *56*, 3320.
- (15) Nalewajski, R. F.; Parr, R. G. *Proc. Natl. Acad. Sci.* **2000**, *97*, 8879.
- (16) Nalewajski, R. F.; Parr, R. G. *J. Phys. Chem. A* **2001**, *105*, 7391.
- (17) Kullback, K.; Leibler, R. A. *Ann. Math. Stat.* **1951**, *22*, 79.
- (18) Politzer, P.; Harris, R. R. *J. Am. Chem. Soc.* **1970**, *92*, 6451.
- (19) Francisco, E.; Martín Pendás, A.; Blanco, M. A. *J. Chem. Theory Comput.* **2006**, *2*, 90.
- (20) Ghosh, D. G.; Biswas, R. *Int. J. Mol. Sci.* **2002**, *3*, 87.
- (21) Schmidt, M. W.; Baldridge, K. K.; Boatz, J. A.; Elbert, S. T.; Gordon, M. S.; Jensen, J. H.; Koseki, S.; Matsunaga, N.; Nguyen, K. A.; Su, S. J.; Windus, T. L.; Dupuis, M.; Montgomery, J. A. *J. Comput. Chem.* **1993**, *14*, 1347.
- (22) Martín Pendás, A.; Blanco, M. A.; Francisco, E. *J. Chem. Phys.* **2004**, *120*, 4581.
- (23) Martín Pendás, A.; Luña, V.; Pueyo, L.; Francisco, E.; Morisánchez, P. *J. Chem. Phys.* **2002**, *117*, 1017.